

Single leptoquark solutions to the B -physics anomalies

Andrei Angelescu^{1,*}, Damir Bečirević^{2,†}, Darius A. Farouhy^{3,‡}, Florentin Jaffredo^{2,§} and Olcyr Sumensari^{2,||}

¹Max-Planck-Institut für Kernphysik, Saupfercheckweg 1, 69117 Heidelberg, Germany

²IJCLab, Pôle Théorie (Bât. 210), CNRS/IN2P3 et Université Paris-Saclay, 91405 Orsay, France

³Physik-Institut, Universität Zürich, CH-8057 Zürich, Switzerland



(Received 26 April 2021; accepted 30 July 2021; published 14 September 2021)

We revisit the possibilities of accommodating the experimental indications of the lepton flavor universality violation in b -hadron decays in the minimal scenarios in which the Standard Model is extended by the presence of a single $\mathcal{O}(1 \text{ TeV})$ leptoquark state. To do so we combine the most recent low energy flavor physics constraints, including $R_{K^{(*)}}^{\text{exp}}$ and $R_{D^{(*)}}^{\text{exp}}$, and combine them with the bounds on the leptoquark masses and their couplings to quarks and leptons as inferred from the direct searches at the LHC and the studies of the large p_T tails of the $pp \rightarrow \ell\ell$ differential cross section. We find that none of the scalar leptoquarks of $m_{LQ} \simeq 1 \div 2 \text{ TeV}$ can accommodate the B -anomalies alone. Only the vector leptoquark, known as U_1 , can provide a viable solution which, in the minimal setup, provides an interesting prediction, i.e., a lower bound to the lepton flavor violating $b \rightarrow s\mu^\pm\tau^\mp$ decay modes, such as $\mathcal{B}(B \rightarrow K\mu\tau) \gtrsim 0.7 \times 10^{-7}$.

DOI: 10.1103/PhysRevD.104.055017

I. INTRODUCTION

In Ref. [1] we made a comprehensive phenomenological analysis of the new physics (NP) scenarios in which the Standard Model (SM) is extended minimally by a single $\mathcal{O}(1 \text{ TeV})$ leptoquark state. The purpose of that study was to examine which one of the known leptoquarks can be made compatible with the experimental indications of the lepton flavor universality violation (LFUV), as inferred from the decays of b -flavored hadrons, and be consistent with many other flavor observables, as well as with the direct and indirect NP searches at the LHC. Since the publication of that study several new measurements appeared, and some of the theoretical estimates have been improved. More specifically:

- (i) LHCb collaboration presented their new result for R_K [2] which now, combined with their previous data, amounts to

$$R_K^{[1.1.6]} = 0.847 \pm 0.042, \quad (1)$$

which is 3.1σ lower than predicted in the SM, $R_K^{[1.6]} = 1.00(1)$ [3].¹ We remind the reader that the ratios

$$R_{K^{(*)}}^{[q_1^2, q_2^2]} = \frac{\mathcal{B}'(B \rightarrow K^{(*)}\mu\mu)}{\mathcal{B}'(B \rightarrow K^{(*)}ee)}, \quad (2)$$

are defined in terms of partial branching fractions (\mathcal{B}'), corresponding to a conveniently chosen interval $q_1^2 \leq q^2 \leq q_2^2$ as to stay away from the prominent $c\bar{c}$ -resonances. In this paper, in addition to the value (1), we will also use [4]

$$\begin{aligned} R_{K^*}^{[0.045, 1.1]} &= 0.68 \pm 0.10, \\ R_{K^*}^{[1.1, 6]} &= 0.71 \pm 0.10. \end{aligned} \quad (3)$$

Notice that a hint of LFUV has also been observed in the decay of Λ_b [5].

- (ii) The experimental value of $\mathcal{B}(B_s \rightarrow \mu\mu)$ has been recently updated to [6]

$$\mathcal{B}(B_s \rightarrow \mu\mu) = (2.70 \pm 0.36) \times 10^{-9}, \quad (4)$$

to which we include the most recent update of the LHCb result $\mathcal{B}(B_s \rightarrow \mu\mu) = (3.09_{-0.44}^{+0.48}) \times 10^{-9}$ [7],

¹We combined the errors in quadrature before symmetrizing them.

*andrei.angelescu@mpi-hd.mpg.de

†damir.becirevic@ijclab.in2p3.fr

‡farouhy@physik.uzh.ch

§florentin.jaffredo@ijclab.in2p3.fr

||olcyr.sumensari@ijclab.in2p3.fr

and by using the prescription of Ref. [8] to build the likelihood functions, the new average value is

$$\mathcal{B}(B_s \rightarrow \mu\mu) = (2.85 \pm 0.33) \times 10^{-9}, \quad (5)$$

thus a little over 2σ lower than predicted in the SM, $\mathcal{B}(B_s \rightarrow \mu\mu) = 3.66(14) \times 10^{-9}$ [9].

- (iii) Experimental indications of LFUV have also been observed in the $b \rightarrow c\ell\bar{\nu}_\ell$ decays, and more specifically in

$$R_{D^{(*)}} = \frac{\mathcal{B}(B \rightarrow D^{(*)}\tau\bar{\nu})}{\mathcal{B}(B \rightarrow D^{(*)}l\bar{\nu})} \Big|_{l \in \{e, \mu\}}. \quad (6)$$

Recent measurements by Belle [10], lead to the new averages [11],

$$\begin{aligned} R_D &= 0.340 \pm 0.030, \\ R_{D^*} &= 0.295 \pm 0.014, \end{aligned} \quad (7)$$

which are, due to experimental correlations, about $\approx 3\sigma$ larger than predicted in the SM (see [11] and references therein),

$$\begin{aligned} R_D^{\text{SM}} &= 0.293 \pm 0.008, \\ R_{D^*}^{\text{SM}} &= 0.257 \pm 0.003. \end{aligned} \quad (8)$$

A similar deviation, but with less competitive experimental uncertainties, has been observed in a similar $R_{J/\psi}$ ratio [12].

- (iv) Direct searches for the leptoquark states, either via the pair production of leptoquarks or through a study of the high p_T tails of the differential cross section of $pp \rightarrow \ell\ell$, have been significantly improved, resulting in ever more stringent bounds on masses and (Yukawa) couplings relevant to the results presented here.

In the following we will use the above experimental improvements, combine them with theoretical expressions used in Ref. [1] and references therein, or with the improved expressions which will be properly referred to in the body of this letter organized as follows: In Sec. II we update the effective field theory (EFT) analysis of the transitions $b \rightarrow s\mu\mu$ and $b \rightarrow c\tau\bar{\nu}$ to determine the effective coefficients that can accommodate the latest experimental results for $R_{K^{(*)}}$ and $R_{D^{(*)}}$. In Sec. III, we remind the reader of the leptoquark (LQ) states that can induce the viable effective operators. In Sec. IV, we derive updated limits on the LQ mass and couplings by using the most recent LHC results at high- p_T . In Sec. V, we combine the low and high-energy constraints to determine which LQs can accommodate the LFU discrepancies. Our findings are summarized in Sec. VI.

II. EFFECTIVE FIELD THEORY

A. R_K and R_{K^*}

The effective Lagrangian for a generic exclusive decay based on $b \rightarrow s\ell_1^-\ell_2^+$, with $\ell_{1,2} \in \{e, \mu, \tau\}$ can be written as

$$\mathcal{L}_{\text{nc}} \supset \frac{4G_F}{\sqrt{2}} V_{tb}V_{ts}^* \sum_i C_i \mathcal{O}_i + \text{H.c.}, \quad (9)$$

where the effective couplings (Wilson coefficients) $C_i \equiv C_i(\mu)$ and the operators $\mathcal{O}_i \equiv \mathcal{O}_i(\mu)$ are defined at the scale μ . The operators relevant to this study are

$$\begin{aligned} \mathcal{O}_9^{\ell_1\ell_2} &= \frac{e^2}{(4\pi)^2} (\bar{s}\gamma_\mu P_L b)(\bar{\ell}_1\gamma^\mu \ell_2), \\ \mathcal{O}_{10}^{\ell_1\ell_2} &= \frac{e^2}{(4\pi)^2} (\bar{s}\gamma_\mu P_L b)(\bar{\ell}_1\gamma^\mu \gamma^5 \ell_2), \\ \mathcal{O}_S^{\ell_1\ell_2} &= \frac{e^2}{(4\pi)^2} (\bar{s}P_R b)(\bar{\ell}_1\ell_2), \\ \mathcal{O}_P^{\ell_1\ell_2} &= \frac{e^2}{(4\pi)^2} (\bar{s}P_R b)(\bar{\ell}_1\gamma^5 \ell_2), \end{aligned} \quad (10)$$

in addition to the chirality flipped ones, \mathcal{O}'_i , obtained from \mathcal{O}_i by replacing $P_L \leftrightarrow P_R$. The effect of operators \mathcal{O}_{1-6} is included in the redefinition of the effective Wilson coefficients $C_{7,9}$. In what follows we ignore the electromagnetic dipole operators $\mathcal{O}_7^{(i)}$ since they do not play a significant role in describing the effects of LFUV. Starting from Eq. (9) it is straightforward to compute the decay rates for $B_s \rightarrow \ell_1^-\ell_2^+$, $B \rightarrow K^{(*)}\ell_1^-\ell_2^+$, and $\Lambda_b \rightarrow \Lambda\ell_1^-\ell_2^+$ see e.g., Refs. [13,14]. In the following the NP contributions to $b \rightarrow s\ell_1^-\ell_2^+$ will be denoted by $\delta C_i^{\ell_1\ell_2}$.

After neglecting the NP couplings to electrons, it has been established that in order to simultaneously accommodate $R_K^{\text{exp}} < R_K^{\text{SM}}$ and $R_{K^*}^{\text{exp}} < R_{K^*}^{\text{SM}}$, the preferred scenarios are those with $\delta C_9^{\mu\mu} < 0$, or those in which $\delta C_9^{\mu\mu} = -\delta C_{10}^{\mu\mu} < 0$. This conclusion has been corroborated by numerous global analyses of the $b \rightarrow s\mu\mu$ observables [15]. In this work, we adopt a conservative approach by only taking into account the LFUV ratios (R_K^{exp} , $R_{K^*}^{\text{exp}}$) and $\mathcal{B}(B_s \rightarrow \mu\mu)^{\text{exp}}$, the quantities for which the hadronic uncertainties are very small and well under control. Notice that the subpercent precision of the lattice QCD determination of the decay constant entering $\mathcal{B}(B_s \rightarrow \mu\mu)^{\text{exp}}$ is also a very recent achievement, $f_{B_s} = 230.3 \pm 1.3$ MeV [16].

²From now on we will drop the electric charges for the LFV modes and denote $\mathcal{B}(B \rightarrow K^{(*)}\ell_1\ell_2) = \mathcal{B}(B \rightarrow K^{(*)}\ell_1^-\ell_2^+) + \mathcal{B}(B \rightarrow K^{(*)}\ell_1^+\ell_2^-)$.

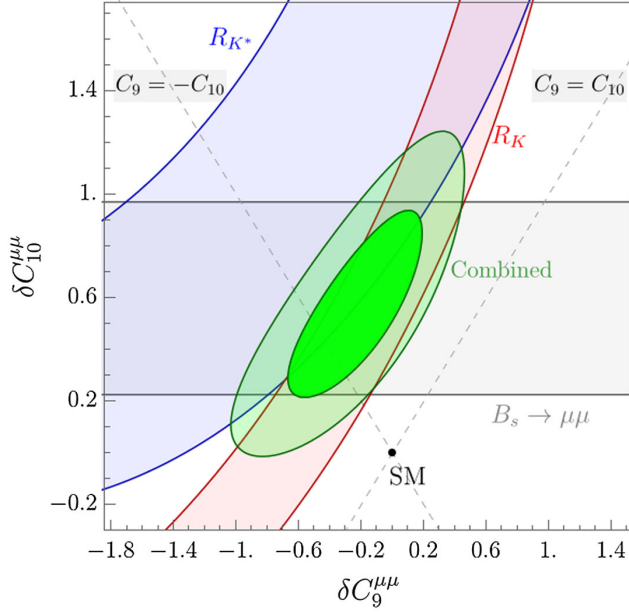


FIG. 1. Allowed regions in the plane $\delta C_9^{\mu\mu}$ vs $\delta C_{10}^{\mu\mu}$ to 1σ accuracy derived by using R_K (red region), R_{K^*} (blue region) and $\mathcal{B}(B_s \rightarrow \mu\mu)$ (gray region). Darker (lighter) green regions correspond to the combined fit to 1σ (2σ) accuracy.

The result of our fit is shown in Fig. 1 where we see a good agreement among all three observables. Furthermore, we again see that the data are not consistent with the scenario $\delta C_9^{\mu\mu} = +\delta C_{10}^{\mu\mu}$, but instead they are consistent with the solution, $\delta C_9^{\mu\mu} = -\delta C_{10}^{\mu\mu}$. By focussing onto the latter, we find

$$\delta C_9^{\mu\mu} = -\delta C_{10}^{\mu\mu} = -0.41 \pm 0.09, \quad (11)$$

which measures the deviation between the measured and the SM predictions of all three observables combined.

B. R_D and R_{D^*}

We remind the reader of the most general low-energy EFT describing the $b \rightarrow c\ell\bar{\nu}$ decay with operators up to dimension-six,

$$\begin{aligned} \mathcal{L}_{cc} = & -2\sqrt{2}G_F V_{cb} [(1 + g_{V_L})(\bar{c}_L \gamma_\mu b_L)(\bar{\ell}_L \gamma^\mu \nu_L) \\ & + g_{V_R}(\bar{c}_R \gamma_\mu b_R)(\bar{\ell}_L \gamma^\mu \nu_L) + g_{S_R}(\bar{c}_L b_R)(\bar{\ell}_R \nu_L) \\ & + g_{S_L}(\bar{c}_R b_L)(\bar{\ell}_R \nu_L) + g_T(\bar{c}_R \sigma_{\mu\nu} b_L)(\bar{\ell}_R \sigma^{\mu\nu} \nu_L)] \\ & + \text{H.c.}, \end{aligned} \quad (12)$$

where the NP couplings, $g_i \equiv g_i(\mu)$, are defined at the renormalization scale which in the following will be taken to be $\mu = m_b$. Flavor indices in g_i are omitted for simplicity.

To determine the allowed values of g_i , we assume that NP predominantly contributes to the $b \rightarrow c\tau\bar{\nu}$ transition, while being tiny in the case of electron or muon in the final

state. In addition to the ratios R_D and R_{D^*} , an important constraint onto $g_P \equiv g_{S_R} - g_{S_L}$ comes from the B_c -meson lifetime [17]. In that respect, we conservatively impose on the still unknown decay rate to be $\mathcal{B}(B_c \rightarrow \tau\bar{\nu}) \lesssim 30\%$. That constraint alone already eliminates a possibility of accommodating the $R_{D^{(*)}}^{\text{exp}}$ values by solely relying on the (pseudo)scalar operators [17].

By using the hadronic input collected in Ref. [1] we make the one-dimensional fits in which one real effective coupling at a time is allowed to take a non-zero value, $g_i(m_b)$, where $i \in \{V_L, S_R, S_L, T\}$. We also consider two scenarios motivated by the LQ models and defined by the relations $g_{S_L}(\Lambda) = +4g_T(\Lambda)$ and $g_{S_L}(\Lambda) = -4g_T(\Lambda)$ at the scale $\Lambda \approx 1$ TeV. After accounting for the renormalization group running from Λ to m_b , these relations become $g_{S_L}(m_b) \approx +8.1g_T(m_b)$ and $g_{S_L}(m_b) \approx -8.5g_T(m_b)$, respectively. We quote the allowed 1σ ranges for $g_{S_L}(m_b)$ in the latter two scenarios, both for real and for purely imaginary values. The results of all these scenarios are presented in Table I, where we see that only a few scenarios can improve the SM description of $b \rightarrow c\tau\bar{\nu}$ data.

In Fig. 2, we predict the correlation between $R_{D^*}/R_{D^*}^{\text{SM}}$ and R_D/R_D^{SM} within selected EFT scenarios, and we confront these predictions with the current experimental values for these ratios. In this plot, we also illustrate the results presented in Table I and confirm that the scenarios with $g_{V_L} > 0$, $g_{S_L} = -4g_T > 0$ and $g_{S_L} = \pm 4g_T \in i\mathbb{R}$ are in good agreement with current data. Furthermore, it becomes clear why the scenario $g_{S_L} = 4g_T \in \mathbb{R}$ is excluded, as it cannot simultaneously explain an excess in both R_D^{exp} and $R_{D^*}^{\text{exp}}$. In the same Fig. 2, we show a similar correlation between $R_{\Lambda_c}/R_{\Lambda_c}^{\text{SM}}$ and $R_{D^*}/R_{D^*}^{\text{SM}}$, which is perhaps more interesting a prediction, since the value of $R_{\Lambda_c} = \mathcal{B}(\Lambda_b \rightarrow \Lambda_c \tau\bar{\nu})/\mathcal{B}(\Lambda_b \rightarrow \Lambda_c \mu\bar{\nu})$ has not yet been experimentally

TABLE I. Low-energy fit to the $b \rightarrow c\tau\bar{\nu}$ effective coefficients (Eff. coeff.) defined in Eq. (12) by using R_D and R_{D^*} , and by imposing that $\mathcal{B}(B_c \rightarrow \tau\bar{\nu}) \lesssim 30\%$. For the individual effective coefficients g_a , we fix the renormalization scale at $\mu = m_b$. For the remaining scenarios with both g_{S_L} and g_T , we impose the conditions $g_{S_L} = \pm 4g_T$ at $\Lambda = 1$ TeV, and provide the allowed range for $g_{S_L}(m_b)$ after accounting for the renormalization-group evolution. The values of χ_{min}^2 for each scenario is to be compared to $\chi_{\text{SM}}^2 = 12.7$.

Eff. coeff.	1σ range	$\chi_{\text{min}}^2/\text{dof}$
$g_{V_L}(m_b)$	0.07 ± 0.02	0.02/1
$g_{S_R}(m_b)$	-0.31 ± 0.05	5.3/1
$g_{S_L}(m_b)$	0.12 ± 0.06	8.8/1
$g_T(m_b)$	-0.03 ± 0.01	3.1/1
$g_{S_L} = +4g_T \in \mathbb{R}$	-0.03 ± 0.07	12.5/1
$g_{S_L} = -4g_T \in \mathbb{R}$	0.16 ± 0.05	2.0/1
$g_{S_L} = \pm 4g_T \in i\mathbb{R}$	0.48 ± 0.08	2.4/1

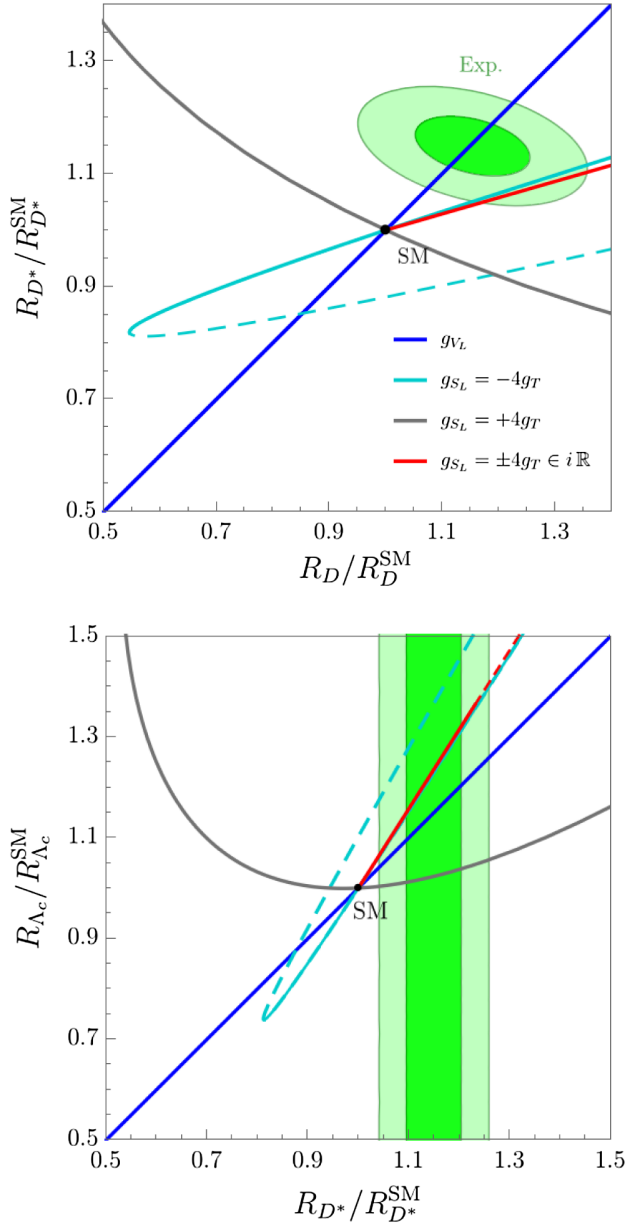


FIG. 2. Predictions for $R_{D^*}/R_{D^*}^{\text{SM}}$ and $R_{\Lambda_c}/R_{\Lambda_c}^{\text{SM}}$ versus R_D/R_D^{SM} in several EFT scenarios, see text for details. Current 1σ (2σ) experimental constraints are depicted by the darker (lighter) green region. Dashed lines correspond to effective couplings that are in tension with the $\mathcal{B}(B_c \rightarrow \tau\nu) < 0.3$ constraint.

established, although the early study has been reported in Ref. [18]. Theoretical expressions for R_{Λ_c} in a general NP scenario (12) can be found in Ref. [19].

III. LEPTOQUARKS FOR $R_{K^{(*)}}$ AND $R_{D^{(*)}}$

In this section we discuss which LQ can be added to the SM in order to accommodate one or both types of the LFUV ratios, $R_{K^{(*)}}$ and $R_{D^{(*)}}$. We refer the reader to our previous paper [1] for a more extensive discussion. We specify each

LQ by its SM quantum numbers ($SU(3)_c, SU(2)_L, U(1)_Y$), where the electric charge, $Q = Y + T_3$, is the sum of the hypercharge (Y) and the third-component of weak isospin (T_3). We neglect the possibility of right-handed neutrinos and we work in the basis with diagonal lepton and down-quark Yukawas, i.e., with left-handed doublets $Q_i = ((V^\dagger u_L)_i; d_{Li})^T$ and $L_i = (\nu_{Li}; \ell_{Li})^T$, where V stands for the CKM matrix.

A. Scalar leptoquarks

- (i) $S_3 = (\bar{\mathbf{3}}, \mathbf{3}, 1/3)$: The weak triplet of LQs is the only scalar boson that can simultaneously accommodate $R_K^{\text{exp}} < R_K^{\text{SM}}$ and $R_{K^*}^{\text{exp}} < R_{K^*}^{\text{SM}}$ at tree level [20,21]. The Yukawa Lagrangian of S_3 can be written as

$$\mathcal{L}_{S_3} = y_L^{ij} \bar{Q}_i^c i\tau_2 (\vec{\tau} \cdot \vec{S}_3) L_j + \text{H.c.}, \quad (13)$$

where τ_k are the Pauli matrices ($k = 1, 2, 3$) and $y_{L(R)}^{ij}$ the generic Yukawa couplings with quark (lepton) indices $i(j)$. LQ couplings to diquarks are neglected in order to guarantee the proton stability [22]. After integrating out the LQ, we find that the $b \rightarrow s \ell \bar{\nu} \ell_k^+$ effective coefficients read

$$\delta C_9^{kl} = -\delta C_{10}^{kl} = \frac{\pi v^2}{V_{tb} V_{ts}^* \alpha_{\text{em}}} \frac{y_L^{bk} (y_L^{sl})^*}{m_{S_3}^2}, \quad (14)$$

which is indeed a pattern that can accommodate $b \rightarrow s \mu \mu$ data, cf. Fig. 1. As for the charged current transitions, $b \rightarrow c \ell \bar{\nu} \ell'$, the S_3 scenario generates at tree level

$$g_{V_L} = -\frac{v^2}{4V_{cb}} \frac{y_L^{b\ell'} (V y_L)_{c\ell}}{m_{S_3}^2}, \quad (15)$$

which is strictly negative if we account for the constraints coming from $B \rightarrow K^{(*)} \nu \bar{\nu}$ and Δm_{B_s} [1]. Therefore, this scenario is in conflict with results presented in Table I and it cannot accommodate $R_{D^{(*)}}^{\text{exp}} > R_{D^{(*)}}^{\text{SM}}$ as a small and positive g_{V_L} value is needed.

- (ii) $S_1 = (\bar{\mathbf{3}}, \mathbf{1}, 1/3)$: The weak singlet scalar LQ has the peculiarity of contributing to the $b \rightarrow c \tau \bar{\nu}$ transition at tree level, but only at loop level to $b \rightarrow s \ell \ell$ [23]. The S_1 Yukawa Lagrangian reads

$$\mathcal{L}_{S_1} = y_L^{ij} \bar{Q}_i^c i\tau_2 L_j S_1 + y_R^{ij} \bar{u}_{Ri}^c \ell_{Rj} S_1 + \text{H.c.}, \quad (16)$$

where y_L and y_R are the LQ Yukawa matrices, and we neglect the diquark couplings for the same reason as in the S_3 case. The coefficients $C_9^{kl} + C_{10}^{kl}$ and $C_9^{kl} - C_{10}^{kl}$ are generated at one-loop by y_L and y_R , respectively, with the relevant expressions provided

in Ref. [23]. This scenario contributes to the $b \rightarrow c\ell\bar{\nu}_{\ell'}$ transitions via,

$$g_{V_L} = \frac{v^2}{4V_{cb}} \frac{y_L^{b\ell'} (Vy_L^*)_{c\ell}}{m_{S_1}^2}, \quad (17)$$

$$g_{S_L} = -4g_T = -\frac{v^2}{4V_{cb}} \frac{y_L^{b\ell'} (y_R^{c\ell'})^*}{m_{S_1}^2}, \quad (18)$$

at the matching scale $\mu = m_{S_1}$. Note, in particular, that both g_{V_L} and $g_{S_L} = -4g_T$ can accommodate the observed excesses in R_D and R_{D^*} , see also Fig. 2.

- (iii) $R_2 = (\mathbf{3}, \mathbf{2}, 7/6)$: The weak doublet was proposed to separately explain the LFUV effects in the charged [24,25] and in the neutral current B -decays [26]. This is the only scalar LQ that automatically conserves baryon number [27]. Its Yukawa Lagrangian writes

$$\mathcal{L}_{R_2} = -y_L^{ij} \bar{u}_{Ri} R_2 i\tau_2 L_j + y_R^{ij} \bar{Q}_i R_2 \ell_{Rj} + \text{H.c.}, \quad (19)$$

with y_L and y_R being the LQ couplings to fermions. At tree level one gets,

$$\delta C_9^{kl} = \delta C_{10}^{kl} \stackrel{\text{tree}}{=} -\frac{\pi v^2}{2V_{tb} V_{ts}^* \alpha_{\text{em}}} \frac{y_R^{sk} (y_R^{bl})^*}{m_{R_2}^2}, \quad (20)$$

a pattern excluded by the observed values of R_K and R_{K^*} , viz. Fig. 1. If, however, one sets $y_R = 0$, the leading contribution to $b \rightarrow s\mu\mu$ arises at one-loop level and the Wilson coefficients verify $\delta C_9^{\mu\mu} = -\delta C_{10}^{\mu\mu} < 0$, which is a satisfactory scenario [26]. Furthermore, this LQ contributes to the transition $b \rightarrow c\ell\bar{\nu}_{\ell'}$, via the effective coupling,

$$g_{S_L} = 4g_T = \frac{v^2}{4V_{cb}} \frac{y_L^{c\ell'} (y_R^{b\ell'})^*}{m_{R_2}^2}, \quad (21)$$

at $\mu = m_{R_2}$. It can therefore accommodate the observed excess in R_D and R_{D^*} , provided a large complex phase is present, cf. Fig. 2.

B. Vector leptoquarks

- (i) $U_1 = (\mathbf{3}, \mathbf{1}, 2/3)$: A scenario with a weak singlet vector LQ attracted a lot of attention in the literature since it provides the operators needed to explain both the $b \rightarrow c\tau\bar{\nu}$ and $b \rightarrow s\mu\mu$ anomalies [28–30]. The corresponding interaction Lagrangian can be written as

$$\mathcal{L}_{U_1} = x_L^{ij} \bar{Q}_i \gamma_\mu L_j U_1^\mu + x_R^{ij} \bar{d}_{Ri} \gamma_\mu \ell_{Rj} U_1^\mu + \text{H.c.}, \quad (22)$$

where x_L and x_R stand for the U_1 couplings to fermions. Notice that the diquark couplings are

absent for this state so that no additional assumption is needed. In its minimal setup, in which $x_R = 0$, and starting from Eq. (22), one can easily obtain the contribution to $b \rightarrow s\ell\bar{\nu}_{\ell'}\ell_k^+$,

$$\delta C_9^{kl} = -\delta C_{10}^{kl} = -\frac{\pi v^2}{V_{tb} V_{ts}^* \alpha_{\text{em}}} \frac{x_L^{sk} (x_L^{bl})^*}{m_{U_1}^2}, \quad (23)$$

while for the $b \rightarrow c\ell\bar{\nu}_{\ell'}$ one gets,

$$g_{V_L} = \frac{v^2}{2V_{cb}} \frac{(Vx_L)_{c\ell'} (x_L^{b\ell'})^*}{m_{U_1}^2}. \quad (24)$$

In other words, this state alone can simultaneously explain $R_{K^{(*)}}$ and $R_{D^{(*)}}$, even in the minimal setup. The main reason for that to be the case is the absence of the tree level constraint coming from $\mathcal{B}(B \rightarrow K^{(*)}\nu\bar{\nu})$.

The challenge for extensions of the SM by a single vector LQ arises at the loop level because this scenario is nonrenormalizable, which then undermines its predictiveness unless the ultraviolet (UV) completion is explicitly specified [31]. Several such completions have been proposed in the literature and they in general involve a Z' and a color-octet of vector bosons, in addition to the U_1 LQ itself, at the $\mathcal{O}(1 \text{ TeV})$ scale [32]. In such situations additional assumptions on the spectrum of these states and on their couplings are required, which is a departure from the minimalistic scenarios described in this paper.

- (ii) $U_3 = (\mathbf{3}, \mathbf{3}, 2/3)$: Finally, the interaction of the weak triplet LQ with quarks and leptons is described by

$$\mathcal{L}_{U_3} = x_L^{ij} \bar{Q}_i \gamma_\mu (\vec{\tau} \cdot \vec{U}_3^\mu) L_j + \text{H.c.}, \quad (25)$$

where, as before, x_L stands for the couplings to fermions. In contrast to U_1 this LQ allows for the dangerous diquark couplings, neglected in the Lagrangian above in order to ensure the proton stability. This scenario contributes to $b \rightarrow s\ell\bar{\nu}_{\ell'}\ell_k^+$ via,

$$\delta C_9^{kl} = -\delta C_{10}^{kl} = -\frac{\pi v^2}{V_{tb} V_{ts}^* \alpha_{\text{em}}} \frac{x_L^{sk} (x_L^{bl})^*}{m_{U_3}^2}, \quad (26)$$

which, again, can explain R_K and R_{K^*} [33], but it contributes to $b \rightarrow c\ell\bar{\nu}_{\ell'}\ell_k^+$ through

$$g_{V_L} = -\frac{v^2}{2V_{cb}} \frac{(Vx_L)_{c\ell'} (x_L^{b\ell'})^*}{m_{U_3}^2}. \quad (27)$$

which is negative and therefore cannot accommodate R_D and R_{D^*} [1], see Table I. Furthermore, being a vector LQ, just like in the case of U_1 , in this

case too it is essential to specify the UV completion in order to remain predictive at the loop level.

IV. LHC CONSTRAINTS

Search for LQs in hadron colliders, either via their direct production [34,35] or through a study of the high- p_T tails of the $pp \rightarrow \ell\ell$ distributions [36–38], results in powerful constraints on the LQ masses and on their couplings to quarks and leptons. We provided such constraints in our previous paper [1], which we update in the following by relying on the most recent LHC data.

A. Direct searches

The dominant mechanism for the LQ production at the LHC is $pp \rightarrow \text{LQ}^\dagger \text{LQ}$. Several searches for LQ pairs have been made at ATLAS and CMS for different final states, namely $(\bar{q}\ell)(q\bar{\ell})$, $(\bar{q}\nu)(q\bar{\nu})$ and $(\bar{q}_d\ell)(q_u\bar{\nu})$, where q_d and q_u stand for the generic down- and up-type quarks. From these searches it is possible to derive model independent bounds on a given LQ mass as a function of its branching fraction into a specific quark-lepton final state.

In Table II we present the new limits on the LQ masses obtained from our recast of the $pp \rightarrow \text{LQ}^\dagger \text{LQ} \rightarrow (\bar{q}\ell)(q\bar{\ell})$ ATLAS and CMS searches. These limits are obtained as a function of the LQ branching fraction β , which we take to the benchmark values $\beta = 1$ and $\beta = 0.5$. Our main assumption is that the LQ production cross-section is dominated by QCD, which is true for the range of Yukawa couplings allowed by flavor constraints [1]. Furthermore, we assume that the vector LQ (V^μ) interaction with gluons ($G^{\mu\nu}$) is described by $\mathcal{L} \supset \kappa g_s V_\mu^\dagger G^{\mu\nu} V_\nu$, with $\kappa = 1$ (Yang-Mills case) [39], and we use the predictions from [35] in our recast. Note that the limits on LQs given in Table II are considerable improvements since our previous study [1], thanks to 140 fb⁻¹ of the LHC data. As a result,

TABLE II. Summary of the current limits from searches for pair-produced LQs at the LHC for possible final states (first column). Limits on scalar and vector LQs are shown in the second and third column, respectively, for a branching fraction $\beta = 1$ ($\beta = 0.5$).

Decays	Scalar LQ limits	Vector LQ limits	$\mathcal{L}_{\text{int}}/\text{Ref.}$
$jj\tau\bar{\tau}$
$b\bar{b}\tau\bar{\tau}$	1.0 (0.8) TeV	1.5 (1.3) TeV	36 fb ⁻¹ [40]
$t\bar{t}\tau\bar{\tau}$	1.4 (1.2) TeV	2.0 (1.8) TeV	140 fb ⁻¹ [41]
$jj\mu\bar{\mu}$	1.7 (1.4) TeV	2.3 (2.1) TeV	140 fb ⁻¹ [42]
$b\bar{b}\mu\bar{\mu}$	1.7 (1.5) TeV	2.3 (2.1) TeV	140 fb ⁻¹ [42]
$t\bar{t}\mu\bar{\mu}$	1.5 (1.3) TeV	2.0 (1.8) TeV	140 fb ⁻¹ [43]
$jj\nu\bar{\nu}$	1.0 (0.6) TeV	1.8 (1.5) TeV	36 fb ⁻¹ [44]
$b\bar{b}\nu\bar{\nu}$	1.1 (0.8) TeV	1.8 (1.5) TeV	36 fb ⁻¹ [44]
$t\bar{t}\nu\bar{\nu}$	1.2 (0.9) TeV	1.8 (1.6) TeV	140 fb ⁻¹ [45]

we see that the overall lower limits on the LQ masses have been increased.

The LHC searches considered in Table II assume that pairs of LQs are produced and decay into the same quark-lepton final states. Recently, CMS performed a search for pair of LQs in the mixed channel $pp \rightarrow \text{LQ}^\dagger \text{LQ} \rightarrow b\tau\nu$, with 140 fb⁻¹ data [46]. This search was performed under the assumption that the LQs decay with equal branching fractions ($\beta = 0.5$) to the final states $\text{LQ}^{(2/3)} \rightarrow b\bar{\tau}, t\bar{\nu}$, or $\text{LQ}^{(-1/3)} \rightarrow t\tau, b\nu$, where the upper index denotes the LQ electric charge. Under this assumption the lower limits 1.0 TeV and 1.8 TeV have been obtained for the scalar and vector LQs, respectively. That search is particularly useful for the $U_1 = (\mathbf{3}, \mathbf{1}, 2/3)$ scenario, since the gauge invariance requirement implies that the couplings of U_1 to $t\bar{\nu}$ and to $b\bar{\tau}$ are equal. Note, however, that this search is very model dependent and, in particular, it does not generically apply to the models containing, e.g., $S_1 = (\bar{\mathbf{3}}, \mathbf{1}, 1/3)$ or $R_2 = (\mathbf{3}, \mathbf{2}, 7/6)$.

B. Bounds from indirect high- p_T searches

Since the pioneering paper of Ref. [36] it is known that the high-energy tails of the invariant mass distribution of the processes $pp \rightarrow \ell\ell^{(\prime)}$ [37,38] and $pp \rightarrow \ell\nu$ [47] are ideal probes for generic LQ models. These observables are particularly useful for setting upper bounds on complementary combinations of the couplings that cannot be constrained by flavor observables at low energies. In order to constrain the LQ couplings using LHC data, we follow a similar recasting procedure as outlined in Ref. [1]. The most recent ATLAS and CMS searches for resonances in the dilepton channels used here are

- (i) $pp \rightarrow \tau^+\tau^-$: We recast the ATLAS search for heavy Higgs boson decaying into the $\tau\tau$ channel, at $\sqrt{s} = 13$ TeV with 140 fb⁻¹ data [48]. We consider events with hadronic τ -leptons (τ_{had}) and we focus our analysis on the b -veto category.
- (ii) $pp \rightarrow \mu^+\mu^-$: We recast the CMS search for a heavy Z' boson decaying into the $\mu\mu$ channel, at $\sqrt{s} = 13$ TeV with 140 fb⁻¹ data [49]

We do not recast LHC searches in the $pp \rightarrow \tau\nu$ mode since they are still only available with 36 fb⁻¹ data [50,51]. Note, in particular, that gauge invariance under $SU(2)_L$ implies that large LQ contributions to $pp \rightarrow \ell\nu$ would necessarily appear in $pp \rightarrow \ell\ell$, which we consider in our study. Moreover, we do not recast the lepton flavor violating (LFV) modes such as $pp \rightarrow \ell\ell'$, with $\ell \neq \ell'$, since these constraints, in the specific case of LQs, turn out to be weaker than the combination of constraints arising from $pp \rightarrow \ell\ell$ and $pp \rightarrow \ell'\ell'$ [1,38].

In this paper, we have refined the procedure for extracting our LQ limits in comparison to our previous paper [1]. The main differences are the following ones:

- (i) We perform a more conservative statistical analysis by using the so-called CL_s method [52].

The 95% confidence level (CL) upper limits on the LQ couplings are obtained by profiling the likelihood ratio with the q_μ test statistics described in [53] and implemented in the `pyhf` package [54]. Notice that the limits extracted using the CL_s method are much more resilient to possible statistical fluctuations in the experimental data populating low sensitivity regions of the spectrum, like, e.g., the tails of the invariant mass. The resulting exclusion limits are therefore weaker when compared to the statistical method employed in [1]. Moreover, when performing the statistical analysis we have included a 20% systematic uncertainty on the LQ signal.

- (ii) We take into account the interference of the t -channel LQ with the SM Drell-Yan process.

Once included, these interference effects can have a moderate impact on the resulting limits, depending on the production channel. In particular, the constructive/destructive interference patterns can strengthen/weaken the naive limits from the $|\mathcal{A}_{\text{NP}}|^2$ term up to $\mathcal{O}(20\%)$.

- (iii) Instead of showing limits from each individual $q\bar{q} \rightarrow \ell\ell$ processes at a time, we provide limits for the individual couplings coming from different production channels. This results in more useful limits on the LQ couplings since they take into account all contributions, including the CKM-suppressed processes. For instance, the limits on the coupling $y_L^{\ell\ell}$ for the S_3 leptoquark are extracted from combining $s\bar{s} \rightarrow \ell\ell$, $c\bar{c} \rightarrow \ell\ell$, and the Cabibbo suppressed processes $u\bar{u}, u\bar{c}, c\bar{u} \rightarrow \ell\ell$.

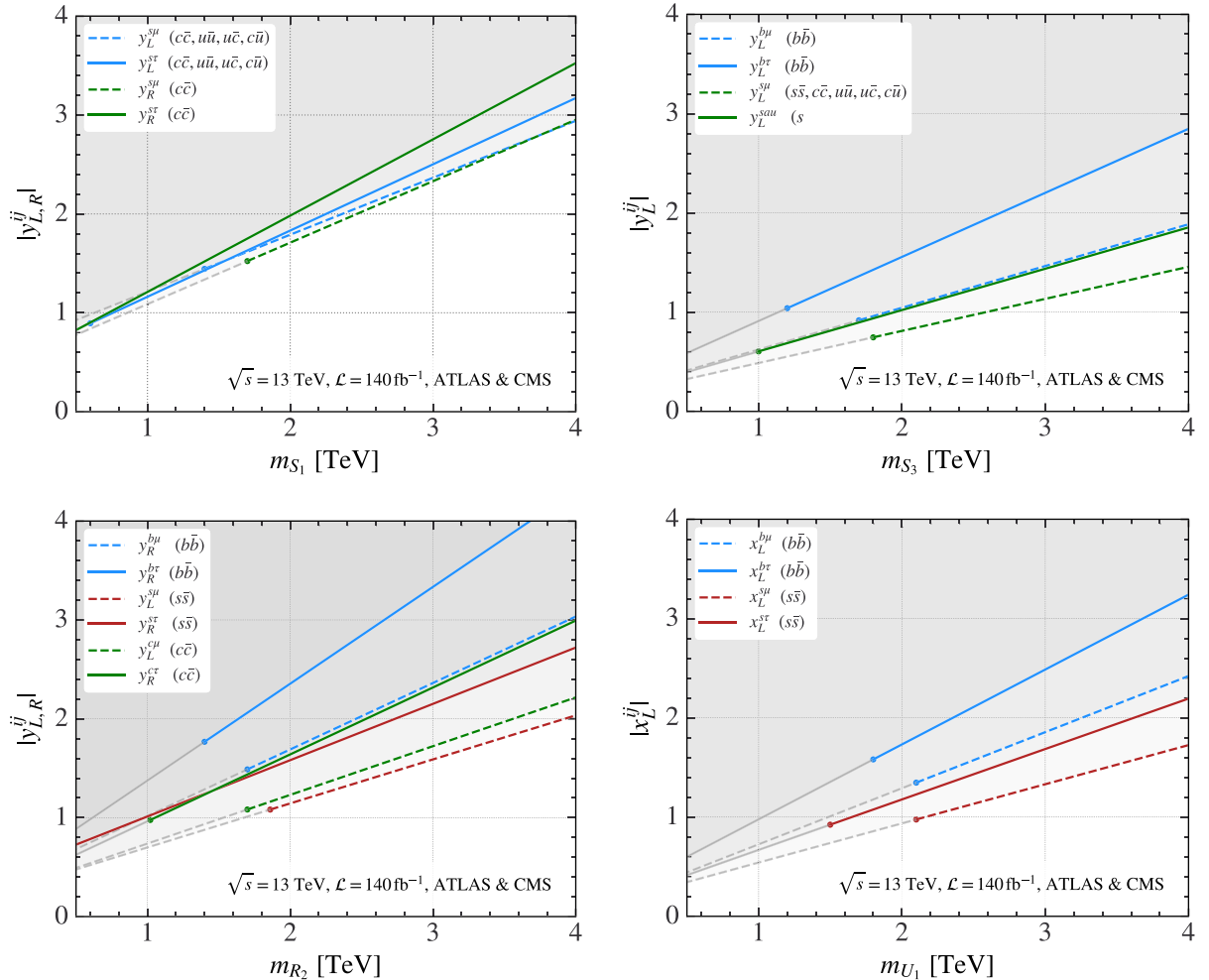


FIG. 3. Upper limits on the scalar (vector) LQ couplings y_L^{ij} (x_L^{ij}), as a function of the LQ masses, which have been obtained from the most recent LHC searches in the high- p_T bins of $pp \rightarrow \ell\ell$ at 13 TeV with 140 fb^{-1} [48,49]. The solid (dashed) lines represent limits arising from di-muon (di-tau) searches, by turning on a single LQ coupling in flavor space. In the plots we highlight the regions consistent with the lower bounds on the LQ masses given in Table II and discussed in Sec. IV A. The $q\bar{q}$ pairs inside the parentheses indicate the combination of $q\bar{q} \rightarrow \ell\ell$ channels used to set the exclusion limits for each coupling. Notice that all $u\bar{u}$ transitions are Cabibbo suppressed.

- (iv) Our limits are also projected to the high-luminosity LHC phase with 3 ab^{-1} in Sec. V. To this purpose, we assume that the signal and background samples scale with the luminosity ratio, whereas all uncertainties scale with its square root. Although this assumption might appear too optimistic, it is worth stressing that higher $m_{\ell\ell}^2$ bins will become available with more data. Those higher bins are more sensitive to the LQ contributions than the bins that have been considered in the searches performed so far [48,49].

Our constraints are collected in Fig. 3 for the LQ models that are relevant for the B -physics anomalies, namely the scalars S_1 , S_3 and R_2 , and the vector U_1 . In these plots we only present limits for the vector LQ couplings to left-handed currents.³ The 95% upper limits on the couplings are obtained as a function of the LQ masses by turning on one single flavor coupling at a time. The specific $q\bar{q} \rightarrow \ell\ell$ transitions contributing to each exclusion limit are displayed inside the parentheses ($q\bar{q}$). As shown in Fig. 3, these limits are typically more stringent than naive perturbative bounds on the couplings, namely $|y| \lesssim \sqrt{4\pi}$. The relevance of these constraints to the scenarios aiming to explain $R_{K^{(*)}}$ and $R_{D^{(*)}}$ will be discussed in Sec. V.

V. WHICH LEPTOQUARK?

In Table III we summarize the situation regarding the viability of a scenario in which the SM is extended by a single $\mathcal{O}(1 \text{ TeV})$ LQ state. We now comment and provide useful information for each one of them.

- (i) S_3 : With respect to our previous paper, the situation in the scenario with a triplet of mass degenerate scalar LQs did not significantly change. This scenario is indeed the best scalar LQ solution to describing the current B -physics anomaly $R_{K^{(*)}}^{\text{exp}} < R_{K^{(*)}}^{\text{SM}}$, which is why it is often combined in the literature with another scalar LQ so as to accommodate both $R_{K^{(*)}}^{\text{exp}} < R_{K^{(*)}}^{\text{SM}}$ and $R_{D^{(*)}}^{\text{exp}} > R_{D^{(*)}}^{\text{SM}}$.
- (ii) S_1 : As noted in Eq. (17), even in the minimalistic scenario (with $y_R^{ij} = 0$), S_1 alone can reproduce the observation $R_{D^{(*)}}^{\text{exp}} > R_{D^{(*)}}^{\text{SM}}$. In the nonminimal case ($y_R^{ij} \neq 0$), the additional coupling, $g_{S_L} = -4g_T$, also provides a viable solution to this problem, cf. Fig. 2. This scenario, however, does not lead to a desired contribution to the $b \rightarrow s\mu\mu$. In the minimal ansatz for the Yukawa couplings accommodating $R_{K^{(*)}}^{\text{exp}} < R_{K^{(*)}}^{\text{SM}}$ and Δm_{B_s} requires large LQ mass, $m_{S_1} \gtrsim 4 \text{ TeV}$, and at least one of the Yukawa couplings to hit the perturbativity limit $\sqrt{4\pi}$ [1]. Therefore, one needs to turn on at least $y_R^{c\tau}$ and otherwise

TABLE III. Summary of the LQ models which can accommodate $R_{K^{(*)}}$ (first column), $R_{D^{(*)}}$ (second column), and both $R_{K^{(*)}}$ and $R_{D^{(*)}}$ (third column), without being in conflict with existing constraints. See text for details.

Model	$R_{K^{(*)}}$	$R_{D^{(*)}}$	$R_{K^{(*)}} \& R_{D^{(*)}}$
S_3 ($\bar{\mathbf{3}}, \mathbf{3}, 1/3$)	✓	✗	✗
S_1 ($\bar{\mathbf{3}}, \mathbf{1}, 1/3$)	✗	✓	✗
R_2 ($\mathbf{3}, \mathbf{2}, 7/6$)	✗	✓	✗
U_1 ($\mathbf{3}, \mathbf{1}, 2/3$)	✓	✓	✓
U_3 ($\mathbf{3}, \mathbf{3}, 2/3$)	✓	✗	✗

satisfy the condition $|y_R^{i\mu}| \ll |y_L^{i\mu}|$, for $i \in \{u, c, t\}$ to be consistent with data, cf. Fig. 1. However, requiring consistency with a number of measured flavor physics observables [1], including $R_{D^{(*)}}^{\mu/e} = \mathcal{B}(B \rightarrow D^{(*)}\mu\bar{\nu})/\mathcal{B}(B \rightarrow D^{(*)}e\bar{\nu})$, $\mathcal{B}(B \rightarrow K^{(*)}\nu\bar{\nu})$, $\mathcal{B}(K \rightarrow \mu\nu)/\mathcal{B}(K \rightarrow e\nu)$ and the experimental limit on $\mathcal{B}(\tau \rightarrow \mu\gamma)$, leads to a large m_{S_1} and very large couplings. This is why the S_1 scenario is considered as unacceptable for describing $R_{K^{(*)}}^{\text{exp}} < R_{K^{(*)}}^{\text{SM}}$, but fully acceptable for describing $R_{D^{(*)}}^{\text{exp}} > R_{D^{(*)}}^{\text{SM}}$. cf. Refs. [1,57,58].

- (iii) R_2 : Clearly, on the basis of Eq. (21) and the results presented in Table I and Fig. 2, this scenario can be viable for enclosing $R_{D^{(*)}}^{\text{exp}} > R_{D^{(*)}}^{\text{SM}}$, if at least one y_R^{ij} is non-zero, usually $y_R^{b\tau}$. In fact, it suffices to allow $y_L^{c\tau}(y_R^{b\tau})^*$ to be $\mathcal{O}(1)$ to ensure the compatibility both with the low-energy observables and with direct searches at LHC, as shown in Fig. 3. As mentioned before, this LQ scenario generates the combination $g_{S_L} = 4g_T$ at the matching scale $\mu \simeq m_{R_2}$, which is consistent with data if g_{S_L} is mostly imaginary, cf. Fig. 2 and Refs. [24,59,60].

Like in the S_1 scenario, this LQ cannot generate the tree level contribution consistent with $R_{K^{(*)}} < R_{K^{(*)}}^{\text{SM}}$, but it can do so through the box-diagrams [26]. The two essential couplings for this to be the case, $y_L^{c\mu}$ and $y_L^{t\mu}$, can now be quantitatively scrutinized. To that end it is enough to use two key constraints: the one arising from the well measured $\mathcal{B}(Z \rightarrow \mu\mu)$ [61] and another one, stemming from the high- p_T tail of the $pp \rightarrow \mu\mu$ differential cross section. Note that the expression for the corresponding LQ contribution to $Z \rightarrow \mu\mu$ has been recently derived in Ref. [62], where the non-negligible finite terms $\propto x_Z \log x_i$ have been properly accounted for ($x_i = m_i^2/m_{R_2}^2$). As for the LQ mass, we use the bound given in Table II and set $m_{R_2} = 1.7 \text{ TeV}$, while from Fig. 3 we can read off the constraints on the couplings as obtained from the large p_T considerations. The result is shown in Fig. 4 where we

³See Refs. [55,56] for recent and updated high- p_T limits for right-handed couplings.

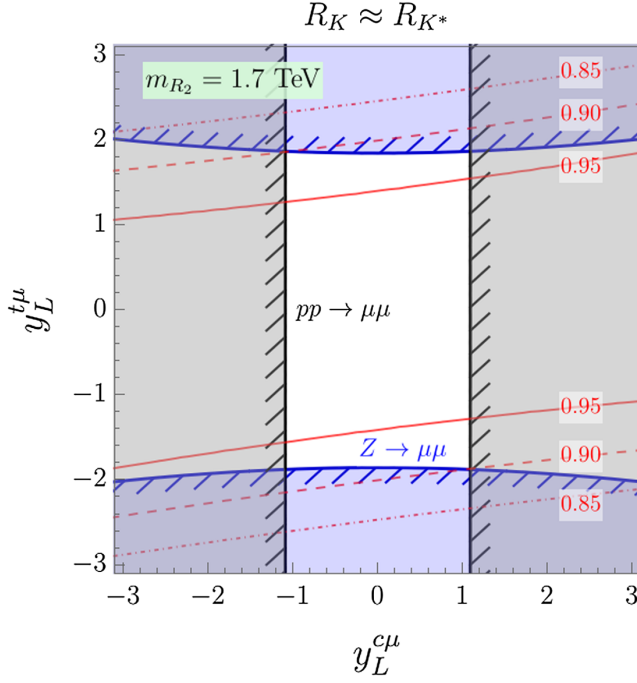


FIG. 4. The allowed regions for the couplings $y_L^{c\mu}$ and $y_L^{t\mu}$ are plotted in white for the $R_2 = (3, 2, 7/6)$ LQ with mass $m_{R_2} = 1.7$ TeV. Predictions for $R_K \approx R_{K^*}$ in the bin $q^2 \in [1, 6]$ GeV² are shown by the red contours. Excluded regions by Z -pole observables and $pp \rightarrow \mu\mu$ constraints are depicted in blue and gray, respectively.

also draw the curves corresponding to three significant values of $R_{K^{(*)}}$, making it obvious that only $R_{K^{(*)}} \gtrsim 0.9$ is compatible with the two mentioned constraints. In other words, $R_{K^{(*)}}$ in this scenario is pushed to the edge of 1σ compatibility with $R_{K^{(*)}}^{(\text{exp})}$, cf. also Ref. [63].

As discussed in our previous paper, the simultaneous explanation of both $R_{K^{(*)}}$ and $R_{D^{(*)}}$ in this

scenario is not possible even to 2σ because of the chiral enhancement by the top quark which leads to a prohibitively large $\mathcal{B}(\tau \rightarrow \mu\gamma)$, in conflict with the experimental bound [26].

- (iv) U_1 : Owing to the fact that this LQ does not contribute to $B \rightarrow K^{(*)}\nu\bar{\nu}$ at tree level, this is the only scenario that can satisfy both anomalies. The main drawback, however, is that the constraints derived from the loop induced processes cannot be used unless a clear UV completion is specified which in turn requires introducing several new parameters and new assumptions (model dependence) making the scenario less predictive. For that reason we do not include, for example, the constraint arising from the frequency of oscillation of the $B_s - \bar{B}_s$ system (Δm_{B_s}) when dealing with vector leptoquarks. In our previous paper [1] we made a detailed analysis and found that this scenario, however, can be significantly constrained by the tree level processes alone, cf. also Ref. [64]. In particular we showed that the model results in interesting correlation between the LFV processes $B \rightarrow K^{(*)}\mu\tau$ and $\tau \rightarrow \mu\phi$, and both the upper and lower bounds for these modes have been derived. With respect to our previous paper, the lower bound on m_{U_1} has increased and we set it to $m_{U_1} = 1.8$ TeV, see Table II. We then use the low energy flavor physics observables as in Ref. [1], combine them with the new constraints on couplings, as obtain from the high- p_T shapes of $pp \rightarrow \ell\ell$, shown in Fig. 3, and instead of plotting the couplings, we focus directly onto observables. Using the expressions for exclusive LFV $b \rightarrow s\ell_1\ell_2$ modes [14,57] in the first panel of Fig. 5 we show how the region of $\mathcal{B}(B \rightarrow K\mu\tau)$ and $\mathcal{B}(\tau \rightarrow \mu\phi)$, allowed by the low-energy flavor physics constraints (gray points), gets reduced to the red region, once the current constraints coming from

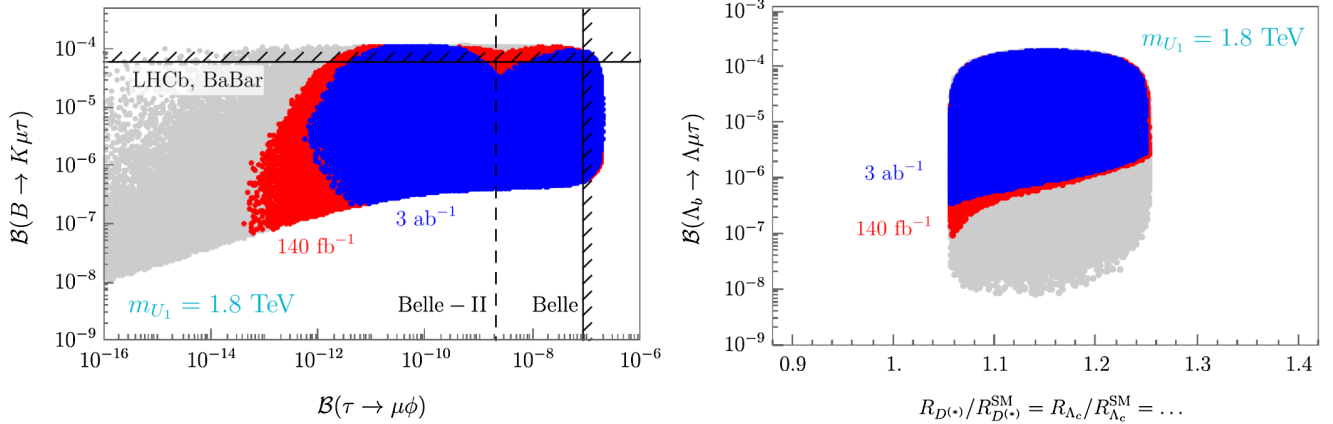


FIG. 5. Lower and upper bounds on the exclusive $b \rightarrow s\mu\tau$ processes as obtained in the minimal U_1 scenario from the constraints arising both from the low-energy observables (gray points) and those coming from the current direct searches at the LHC (red points), the subset of which (blue points) correspond to the projected integrated luminosity of 3 ab^{-1} .

the high p_T considerations of $pp \rightarrow \ell\ell$ at the LHC are taken into account. We see that in both channels the current experimental bounds are already eliminating small sections of the parameter space. In the same plot we also show how that experimental bound on $\mathcal{B}(\tau \rightarrow \mu\phi)$ is expected to be lowered once the Belle II runs will be completed [65]. Concerning the experimental bound on $\mathcal{B}(B \rightarrow K\mu\tau)$, we note that the BABAR bound (4.8×10^{-5}) [66] has been recently confirmed and slightly improved by LHCb (3.9×10^{-5}) [67]. In the minimal U_1 scenario considered here, and with the current experimental constraints, we obtain

$$\mathcal{B}(B \rightarrow K\mu\tau) \gtrsim 0.7 \times 10^{-7}, \quad (28)$$

which could be tested experimentally. Note that this (lower) bound is not expected to increase significantly with the improved luminosity of the LHC data, and with the projected 3 ab^{-1} of data we get only a factor of about 3 improvement, namely $\mathcal{B}(B \rightarrow K\mu\tau) \gtrsim 2.2 \times 10^{-7}$.

We should also mention that, in this scenario, from the lower bound (28) and the experimental upper bound, one can derive the bounds on similar decay modes since $\mathcal{B}(B \rightarrow K^*\mu\tau)/\mathcal{B}(B \rightarrow K\mu\tau) \approx 1.8$, $\mathcal{B}(B_s \rightarrow \mu\tau)/\mathcal{B}(B \rightarrow K\mu\tau) \approx 0.9$, and $\mathcal{B}(\Lambda_b \rightarrow \Lambda\mu\tau)/\mathcal{B}(B \rightarrow K\mu\tau) \approx 1.7$ [14]. Furthermore, in this scenario the SM contribution to the $b \rightarrow c\tau\bar{\nu}$ decay modes gets only modified by and overall factor. For that reason, the predicted increase of R_X with respect to the SM is the same for any $X \in \{D^{(*)}, D_s^{(*)}, J/\psi, \Lambda_c^{(*)}, \dots\}$. From the right panel of Fig. 5 we see that with the current experimental constraints we have

$$1.05 \lesssim \frac{R_X}{R_X^{\text{SM}}} \lesssim 1.25, \quad (29)$$

the interval which remains as such even by projecting to 3 ab^{-1} of the LHC data (blue regions in Fig. 5).

We were able to check the robustness of the above findings by varying m_{U_1} and by imposing all of the constraints mentioned above, including the LHC bounds on the pair-produced leptoquarks decaying into various final states. The result is shown in Fig. 6 from which we see that the lower bound on $\mathcal{B}(B \rightarrow K\mu\tau)$ remains stable with respect to the variation of m_{U_1} . Notice that the lower bound on the mass is $m_{U_1} \gtrsim 1.35 \text{ TeV}$, while the perturbativity limit on the couplings set an upper limit $m_{U_1} \lesssim 18 \text{ TeV}$.

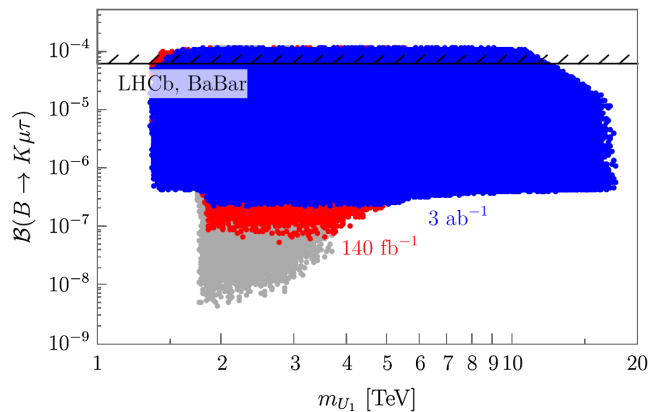


FIG. 6. Limits on $\mathcal{B}(B \rightarrow K\mu\tau)$ with respect to the variation of the mass of the U_1 -leptoquark, and by keeping all of the constraints discussed in the text. Colors of the points are the same as in Fig. 5.

VI. CONCLUSIONS

In this work we revisited our previous phenomenological study and examined the viability of the scenarios in which the SM is extended by only one $\mathcal{O}(1 \text{ TeV})$ LQ after comparing them to the most recent experimental results, in addition to those already discussed in our Ref. [1]. In that respect the Belle measurement of $R_{D^{(*)}}$ [10] has been particularly important, as well as the new R_K and $\mathcal{B}(B_s \rightarrow \mu\mu)$ values reported by the LHCb Collaboration [2,7]. Besides the low-energy observables, we also exploit the most recent experimental improvements regarding the direct searches and the high p_T considerations of the $pp \rightarrow \ell\ell$ differential cross section studied at the LHC.

Better experimental bounds on the LQ pair production, $pp \rightarrow \text{LQ}^+\text{LQ}$, results in a larger lower bound on m_{LQ} , now straddling 2 TeV and being higher for the vector LQs than that for the scalar ones. From the study of the large- p_T spectrum of the differential cross section of $pp \rightarrow \ell\ell$, we extract the upper bounds on Yukawa couplings which provide us with constraints complementary to those inferred from the low-energy observables.

Whenever available we use the improved theoretical expressions and improved hadronic inputs. On the basis of our results, which are summarized in Table III, we confirm that none of the scalar LQs alone, with the mass $m_{\text{LQ}} \lesssim 2 \text{ TeV}$, can be a viable scenario of NP that captures both types of anomalies, $R_{K^{(*)}}^{\text{exp}} < R_{K^{(*)}}^{\text{SM}}$ and $R_{D^{(*)}}^{\text{exp}} > R_{D^{(*)}}^{\text{SM}}$. Instead, one can combine S_3 with either S_1 or R_2 [25,68–70] to get a model suitable for describing all of the data in a scenario requiring the least number of parameters.

With the new experimental data we were able to better examine the model with R_2 scalar LQ, and check on the possibility of describing the $R_{K^{(*)}}^{\text{exp}} < R_{K^{(*)}}^{\text{SM}}$ anomaly through the loop process. We found that $\mathcal{B}(Z \rightarrow \mu\mu)$ and the constraint coming from the high p_T shape of the $pp \rightarrow \mu\mu$ cross section at the LHC are complementary to each

other and allow us to rule out the model (to 1σ) if $R_{K^{(*)}} \lesssim 0.9$.

Besides the scalar LQs we also considered the vector one, U_1 , for which we could not account for the loop induced processes, such as Δm_{B_s} , but by focusing on the tree level observables alone we could confirm that this scenario, in its minimal setup ($x_R = 0$) can describe both $R_{D^{(*)}}^{\text{exp}} > R_{D^{(*)}}^{\text{SM}}$ and $R_{K^{(*)}}^{\text{exp}} < R_{K^{(*)}}^{\text{SM}}$. In this U_1 model all the exclusive processes based on $b \rightarrow c\tau\bar{\nu}$ are modified by the same multiplicative factor so that all the LFUV ratios are the same. In other words, and with the currently available experimental information, $1.05 \lesssim R_X/R_X^{\text{SM}} \lesssim 1.25$, $X \in \{D^{(*)}, D_s^{(*)}, J/\psi, \Lambda_c^{(*)}, \dots\}$. Also interesting are the upper and lower bounds on the LFV $b \rightarrow s\mu\tau$ modes. While the upper bound is already superseded by the experimentally established one, this scenario provides us with the lower bound, which we found to be $\mathcal{B}(B \rightarrow K\mu\tau) \gtrsim 0.7 \times 10^{-7}$.

In this study we also included baryons and obtain $1.2 \times 10^{-7} \lesssim \mathcal{B}(\Lambda_b \rightarrow \Lambda\mu\tau) \lesssim 6.6 \times 10^{-5}$, where the lower bound is a prediction of the U_1 model discussed here, and the upper bound is obtained by rescaling the experimental bound on $\mathcal{B}(B \rightarrow K\mu\tau)$.

ACKNOWLEDGMENTS

This project has received support from the European Union's Horizon 2020 research and innovation programme under the Marie Skłodowska-Curie Grant agreement No. 860881-HIDDeN. The work of D. A. F. has received funding from the European Research Council (ERC) under the European Union's Horizon 2020 research and innovation programme under Grant agreement No. 833280 (FLAY), and by the Swiss National Science Foundation (SNF) under Contract No. 200021-175940.

-
- [1] A. Angelescu, D. Bečirević, D. A. Faroughy, and O. Sumensari, *J. High Energy Phys.* **10** (2018) 183.
- [2] R. Aaij *et al.* (LHCb Collaboration), arXiv:2103.11769.
- [3] M. Bordone, G. Isidori, and A. Pattori, *Eur. Phys. J. C* **76**, 440 (2016); G. Isidori, S. Nabeebaccus, and R. Zwicky, *J. High Energy Phys.* **12** (2020) 104.
- [4] R. Aaij *et al.* (LHCb Collaboration), *J. High Energy Phys.* **08** (2017) 055.
- [5] R. Aaij *et al.* (LHCb Collaboration), *J. High Energy Phys.* **05** (2020) 040.
- [6] The ATLAS, CMS and LHCb Collaborations, Report No. CMS-PAS-BPH-20-003.
- [7] F. Archilli (LHCb Collaboration), Proceedings of the 55th Rencontres de Moriond 2021, Electroweak Interactions and Unified Theories, 2021, http://moriond.in2p3.fr/2021/EW/slides/3_flavour_01_archilli.pdf.
- [8] R. Barlow, arXiv:physics/0406120.
- [9] M. Beneke, C. Bobeth, and R. Szafron, *J. High Energy Phys.* **10** (2019) 232.
- [10] A. Abdesselam *et al.* (Belle Collaboration), arXiv:1904.08794.
- [11] Y. S. Amhis *et al.* (HFLAV Collaboration), *Eur. Phys. J. C* **81**, 226 (2021); on-line updates can be found at <https://hflav.web.cern.ch/>.
- [12] R. Aaij *et al.* (LHCb Collaboration), *Phys. Rev. Lett.* **120**, 121801 (2018).
- [13] D. Bečirević, O. Sumensari, and R. Z. Funchal, *Eur. Phys. J. C* **76**, 134 (2016).
- [14] D. Becirevic, S. Fajfer, F. Jaffredo, and O. Sumensari (to be published).
- [15] B. Capdevila, A. Crivellin, S. Descotes-Genon, J. Matias, and J. Virto, *J. High Energy Phys.* **01** (2018) 093; G. D'Amico, M. Nardecchia, P. Panci, F. Sannino, A. Strumia, R. Torre, and A. Urbano, *J. High Energy Phys.* **09** (2017) 010; W. Altmannshofer, P. Stangl, and D. M. Straub, *Phys. Rev. D* **96**, 055008 (2017); arXiv:2103.13370; M. Ciuchini, A. M. Coutinho, M. Fedele, E. Franco, A. Paul, L. Silvestrini, and M. Valli, *Eur. Phys. J. C* **79**, 719 (2019); *Phys. Rev. D* **103**, 015030 (2021); T. Hurth, F. Mahmoudi, D. M. Santos, and S. Neshatpour, *Phys. Rev. D* **96**, 095034 (2017); A. K. Alok, B. Bhattacharya, A. Datta, D. Kumar, J. Kumar, and D. London, *Phys. Rev. D* **96**, 095009 (2017).
- [16] S. Aoki *et al.* (Flavour Lattice Averaging Group Collaboration), *Eur. Phys. J. C* **80**, 113 (2020).
- [17] X. Q. Li, Y. D. Yang, and X. Zhang, *J. High Energy Phys.* **08** (2016) 054; R. Alonso, B. Grinstein, and J. M. Camalich, *Phys. Rev. Lett.* **118**, 081802 (2017); A. Celis, M. Jung, X. Q. Li, and A. Pich, *Phys. Lett. B* **771**, 168 (2017).
- [18] V. Daussy-Renaudin, Probing lepton flavour universality through semitauonic Λ_b decays using three-pions τ -lepton decays with the LHCb experiment at CERN, Ph.D thesis, <http://www.theses.fr/2018SACL335>.
- [19] P. Böer, A. Kokulu, J. N. Toelstede, and D. van Dyk, *J. High Energy Phys.* **12** (2019) 082; A. Datta, S. Kamali, S. Meinel, and A. Rashed, *J. High Energy Phys.* **08** (2017) 131; X. Q. Li, Y. D. Yang, and X. Zhang, *J. High Energy Phys.* **08** (2016) 054; X. L. Mu, Y. Li, Z. T. Zou, and B. Zhu, *Phys. Rev. D* **100**, 113004 (2019); N. Penalva, E. Hernández, and J. Nieves, *Phys. Rev. D* **101**, 113004 (2020); D. Becirevic and F. Jaffredo (to be published).
- [20] G. Hiller and M. Schmaltz, *Phys. Rev. D* **90**, 054014 (2014); G. Hiller and I. Nisandzic, *Phys. Rev. D* **96**, 035003 (2017).
- [21] I. Doršner, S. Fajfer, D. A. Faroughy, and N. Košnik, *J. High Energy Phys.* **10** (2017) 188.
- [22] I. Doršner, S. Fajfer, A. Greljo, J. F. Kamenik, and N. Košnik, *Phys. Rep.* **641**, 1 (2016).
- [23] M. Bauer and M. Neubert, *Phys. Rev. Lett.* **116**, 141802 (2016).

- [24] Y. Sakaki, R. Watanabe, M. Tanaka, and A. Tayduganov, *Phys. Rev. D* **88**, 094012 (2013).
- [25] D. Bečirević, I. Doršner, S. Fajfer, D. A. Faroughy, N. Košnik, and O. Sumensari, *Phys. Rev. D* **98**, 055003 (2018).
- [26] D. Bečirević and O. Sumensari, *J. High Energy Phys.* **08** (2017) 104.
- [27] N. Assad, B. Fornal, and B. Grinstein, *Phys. Lett. B* **777**, 324 (2018).
- [28] R. Alonso, B. Grinstein, and J. M. Camalich, *J. High Energy Phys.* **10** (2015) 184; L. Calibbi, A. Crivellin, and T. Ota, *Phys. Rev. Lett.* **115**, 181801 (2015).
- [29] D. Buttazzo, A. Greljo, G. Isidori, and D. Marzocca, *J. High Energy Phys.* **11** (2017) 044.
- [30] J. Kumar, D. London, and R. Watanabe, *Phys. Rev. D* **99**, 015007 (2019); A. K. Alok, B. Bhattacharya, A. Datta, D. Kumar, J. Kumar, and D. London, *Phys. Rev. D* **96**, 095009 (2017).
- [31] R. Barbieri, G. Isidori, A. Pattori, and F. Senia, *Eur. Phys. J. C* **76**, 67 (2016).
- [32] L. Di Luzio, A. Greljo, and M. Nardecchia, *Phys. Rev. D* **96**, 115011 (2017); L. Di Luzio, J. Fuentes-Martín, A. Greljo, M. Nardecchia, and S. Renner, *J. High Energy Phys.* **11** (2018) 081; M. Bordone, C. Cornella, J. Fuentes-Martín, and G. Isidori, *Phys. Lett. B* **779**, 317 (2018); R. Barbieri and A. Tesi, *Eur. Phys. J. C* **78**, 193 (2018); L. Calibbi, A. Crivellin, and T. Li, *Phys. Rev. D* **98**, 115002 (2018); M. Blanke and A. Crivellin, *Phys. Rev. Lett.* **121**, 011801 (2018); J. Fuentes-Martín and P. Stangl, *Phys. Lett. B* **811**, 135953 (2020).
- [33] S. Fajfer and N. Košnik, *Phys. Lett. B* **755**, 270 (2016); A. Bhaskar, D. Das, T. Mandal, S. Mitra, and C. Neeraj, *arXiv*: 2101.12069.
- [34] B. Diaz, M. Schmaltz, and Y. M. Zhong, *J. High Energy Phys.* **10** (2017) 097.
- [35] I. Doršner and A. Greljo, *J. High Energy Phys.* **05** (2018) 126.
- [36] O. J. P. Eboli and A. V. Olinto, *Phys. Rev. D* **38**, 3461 (1988).
- [37] D. A. Faroughy, A. Greljo, and J. F. Kamenik, *Phys. Lett. B* **764**, 126 (2017); M. Schmaltz and Y. M. Zhong, *J. High Energy Phys.* **01** (2019) 132; A. Greljo and D. Marzocca, *Eur. Phys. J. C* **77**, 548 (2017); A. Alves, O. J. P. Eboli, G. G. di Cortona, and R. R. Moreira, *Phys. Rev. D* **99**, 095005 (2019); Y. Afik, S. Bar-Shalom, J. Cohen, and Y. Rozen, *Phys. Lett. B* **807**, 135541 (2020).
- [38] A. Angelescu, D. A. Faroughy, and O. Sumensari, *Eur. Phys. J. C* **80**, 641 (2020).
- [39] J. Blumlein, E. Boos, and A. Kryukov, *Z. Phys. C* **76**, 137 (1997).
- [40] M. Aaboud *et al.* (ATLAS Collaboration), *J. High Energy Phys.* **06** (2019) 144.
- [41] G. Aad *et al.* (ATLAS Collaboration), *J. High Energy Phys.* **06** (2021) 179.
- [42] G. Aad *et al.* (ATLAS Collaboration), *J. High Energy Phys.* **10** (2020) 112.
- [43] G. Aad *et al.* (ATLAS Collaboration), *Eur. Phys. J. C* **81**, 313 (2021).
- [44] The CMS Collaboration, Report No. CMS-PAS-SUS-18-001.
- [45] G. Aad *et al.* (ATLAS Collaboration), *Eur. Phys. J. C* **80**, 737 (2020).
- [46] A. M. Sirunyan *et al.* (CMS Collaboration), *Phys. Lett. B* **819**, 136446 (2021).
- [47] T. Mandal, S. Mitra, and S. Raz, *Phys. Rev. D* **99**, 055028 (2019); A. Greljo, J. M. Camalich, and J. D. Ruiz-Álvarez, *Phys. Rev. Lett.* **122**, 131803 (2019); D. Marzocca, U. Min, and M. Son, *J. High Energy Phys.* **12** (2020) 035.
- [48] G. Aad *et al.* (ATLAS Collaboration), *Phys. Rev. Lett.* **125**, 051801 (2020).
- [49] The CMS Collaboration, Report No. CMS-PAS-EXO-19-019.
- [50] A. M. Sirunyan *et al.* (CMS Collaboration), *Phys. Lett. B* **792**, 107 (2019).
- [51] M. Aaboud *et al.* (ATLAS Collaboration), *Phys. Rev. Lett.* **120**, 161802 (2018).
- [52] A. L. Read, *J. Phys. G* **28**, 2693 (2002).
- [53] G. Cowan, K. Cranmer, E. Gross, and O. Vitells, *Eur. Phys. J. C* **71**, 1554 (2011); **73**, 2501(E) (2013).
- [54] L. Heinrich, M. Feickert, and G. Stark. (2020). scikit-hep/pyhf: v0.4.3 (Version v0.4.3). Zenodo, <http://doi.org/10.5281/zenodo.3870990>.
- [55] M. Baker, J. Fuentes-Martín, G. Isidori, and M. König, *Eur. Phys. J. C* **79**, 334 (2019).
- [56] C. Cornella, D. A. Faroughy, J. Fuentes-Martín, G. Isidori, and M. Neubert, *arXiv*:2103.16558.
- [57] D. Bečirević, N. Košnik, O. Sumensari, and R. Z. Funchal, *J. High Energy Phys.* **11** (2016) 035.
- [58] Y. Cai, J. Gargalionis, M. A. Schmidt, and R. R. Volkas, *J. High Energy Phys.* **10** (2017) 047.
- [59] D. Bečirević, B. Panes, O. Sumensari, and R. Z. Funchal, *J. High Energy Phys.* **06** (2018) 032.
- [60] G. Hiller, D. Loose, and K. Schönwald, *J. High Energy Phys.* **12** (2016) 027.
- [61] P. A. Zyla *et al.* (Particle Data Group Collaboration), *Prog. Theor. Exp. Phys.* **2020**, 083C01 (2020).
- [62] P. Arnan, D. Becirevic, F. Mescia, and O. Sumensari, *J. High Energy Phys.* **02** (2019) 109.
- [63] J. E. Camargo-Molina, A. Celis, and D. A. Faroughy, *Phys. Lett. B* **784**, 284 (2018); R. Coy, M. Frigerio, F. Mescia, and O. Sumensari, *Eur. Phys. J. C* **80**, 52 (2020).
- [64] C. Cornella, J. Fuentes-Martín, and G. Isidori, *J. High Energy Phys.* **07** (2019) 168.
- [65] E. Kou *et al.* (Belle-II Collaboration), *Prog. Theor. Exp. Phys.* **2019**, 123C01 (2019); **2020**, 029201(E) (2020).
- [66] J. P. Lees *et al.* (BABAR Collaboration), *Phys. Rev. D* **86**, 012004 (2012).
- [67] R. Aaij *et al.* (LHCb Collaboration), *J. High Energy Phys.* **06** (2020) 129.
- [68] S. Saad and A. Thapa, *Phys. Rev. D* **102**, 015014 (2020); K. S. Babu, P. S. B. Dev, S. Jana, and A. Thapa, *J. High Energy Phys.* **03** (2021) 179.
- [69] V. Gherardi, D. Marzocca, and E. Venturini, *J. High Energy Phys.* **01** (2021) 138; D. Marzocca, *J. High Energy Phys.* **07** (2018) 121.
- [70] A. Crivellin, D. Müller, and T. Ota, *J. High Energy Phys.* **09** (2017) 040; A. Crivellin, D. Müller, and F. Saturnino, *J. High Energy Phys.* **06** (2020) 020.